P9.6 A NEW DEALIASING METHOD FOR DOPPLER VELOCITY DATA QUALITY CONTROL

Qin Xu[1]*, [2], Kang Nai[2], Pengfei Zhang[2], Shun Liu[3] and David Parrish[3]

[1]NOAA/National Severe Storms Laboratory, Norman, Oklahoma
[2]Cooperative Institute for Mesoscale Meteorological Studies, University of Oklahoma
[3]NOAA/National Centers of Environmental Prediction, Camp Springs, Maryland

1. INTRODUCTION

It has been increasingly well recognized in recent years that radar data quality control is critical for radar data assimilation. To support the operational radar data assimilation at the National Centers of Environmental Prediction (NCEP), continued efforts have been made in developing efficient quality control techniques for Doppler radial-velocity observations from operational WSR-88D radars (Gong *et al.* 2003; Liu et al. 2005; Zhang et al. 2005; Xu et al. 2009a,c). The earlier developed techniques were combined into an automated quality control package for pre-operational tests with real-time KTLX radar observations at NSSL (Liu et al. 2003; Xu et al. 2005) and then operational tests at NCEP (Liu et al. 2009). During the tests, some particularly difficult cases were encountered in which the three-step dealiasing method (Gong *et al.* 2003) failed to detect or correct severely aliased radial-velocities. Having diagnosed each failure in details, the following two reasons have been identified. (i) The modified velocity azimuth display (VAD) technique (Tabary *et al.* 2001) adopted in the first step is not sufficiently robust to deal with severely aliased radial velocities, so the refined reference radial velocities produced by the traditional VAD method in the second step cannot always ensure the seed data qualified at the end of the second step to be absolutely free of alias errors, and the errors can propagate via the point-to-point continuity check in the third step. (ii) The point-to-point continuity check in the third step relies on qualified seed data, and it cannot pass a non-qualified date area (including data holes) that has 5 or more gates (2.5 km) along the previous and current beams from the flagged data point that is being checked. Besides, the point-to-point continuity check may also occasionally produce false dealiasing and propagate the error into neighborhood areas.

To eliminate the above sources of dealiasing failure, an alias-robust VAD algorithm was developed (Xu *et al.* 2009b) and is used to replace the modified VAD method for the preliminary reference check in the first step. After this, the traditional VAD analysis and refined reference check in the second step becomes unnecessary and thus can be bypassed. In addition, a block-to-point continuity check is designed to replace the point-to-point continuity check in the third step of the three-step dealiasing method (Gong *et al.*, 2003). With these major upgrades, the performance and robustness of the method are greatly improved. The new method is described in the next section.

* Corresponding author address: Qin Xu, National Severe Storms Laboratory, 120 David L. Boren Blvd., Norman, OK 73072-7326; E-mail: Qin.Xu@noaa.gov

2. DESCRIPTION OF THE METHOD

2.1. First Step – Reference Check

In the first step, the alias-robust VAD algorithm (described in section 4.3 of Xu *et al.*, 2009b) is used to estimate the vertical profile of the horizontal vector wind, denoted by (u_0, v_0), averaged over the horizontal area covered by the radar radial-velocity observations. The VAD wind direction is derived from the two zero points of $v_r(\phi)$ searched and estimated on each qualified vertical level, where $v_r(\phi)$ denotes the true radial velocity as a function of the azimuthal angle ϕ (clockwise with respect to the y-coordinate pointing to the north). In the presence of aliasing, the observed radial velocities can become nearly zero over a small azimuthal range which often contains an aliased zero point. The absolute value of the azimuthal derivative estimated at such an aliased zero point should be smaller than that estimated at the true zero point (where the azimuthal derivative has the same sign as that at the aliased zero point), and this criterion can be used to distinguish the two true zero points from aliased zero points (see section 2.4 of Xu *et al.*, 2009b). Occasionally, however, observed radial velocities can be contaminated to become falsely near zero over an azimuthally extended sector and therefore interfere the searching for the true zero points. Thus, before the first step starts, the data need to be preprocessed to remove isolated data points (as in Gong *et al.*, 2003) and flag near-zero radial-velocity sectors. The detailed sub-steps are reported in Xu *et al.* (2009a).

The parameters estimated by the alias-robust VAD algorithm from a selected range circle include not only the averaged horizontal vector wind (u_0, v_0) but also $a_0 = (w - w_T)_0 \sin\theta + r\cos^2\theta(\partial u/\partial x + \partial v/\partial y)_0/2$ [see Eq. (1) below], where θ is the elevation angle, r is

the radial range of the circle, w is the air motion vertical velocity, w_T is the downward hydrometeors terminal fall velocity, $\partial u/\partial x + \partial v/\partial y$ is the divergence of the horizontal wind, and $(\ )_0$ denotes the averaged value of ( ) over the horizontal area covered by the radar radial-velocity observations. As described in section 4.3 of Xu *et al*. (2009b), these parameters are estimated at each qualified vertical level by using all the observations on the qualified and semi-qualified range circles from different tilts.

Once the VAD parameters (a_0, u_0, v_0) estimated at the qualified vertical levels are interpolated to the vertical level of a selected range circle on a given tilt, the reference radial velocity is computed at each observation point on the selected range circle by the following relationship [see (2) of Xu *et al*., 2009b]:

$$v_r^{ref} = a_0 + \cos\theta(u_0\sin\phi + v_0\cos\phi). \quad (1)$$

The computed v_r is used for the preliminary reference check. The check goes through each data point along each circle, from the smallest circle on each tilt until it reaches the largest radial range (corresponding to the top vertical level attained by the VAD analysis) or the cut-off radial range (r = 30 km if $\theta \approx 0.5^\circ$ or r = 80 km if $\theta \geq 1^\circ$) whichever is reached first. The cut-off radial ranges (30 km for $\theta \approx 0.5^\circ$ and 80 km for $\theta \geq 1^\circ$) are new for the upgraded reference check in the paper, and they are imposed to avoid possible false dealiasing (caused by the deteriorated validity of the VAD uniform-wind assumption at an increasingly far radial range in a scenario of strongly non-uniform wind). Their values are tuned and selected based on our extensive tests of the new method. In addition, the alias correction threshold used by the upgraded reference check here is more stringent than used by the reference check in the three-step method (Gong *et al*., 2003). In particular, the Nyquist folding number is estimated by

$$N = \mathrm{Int}[(v_r^{ref} - v_r^o)/2v_N], \quad (2)$$

where $\mathrm{Int}[(\ )/2v_N]$ represents the nearest integer of $(\ )/2v_N$, v_r^o is the observed radial velocity, and v_N is the Nyquist velocity. If N = 0, then the observed radial velocity needs no correction, but it can pass the reference check only if $|v_r^{ref} - v_r^o| \leq 0.5v_N$, If $N \neq 0$, then $2Nv_N$ is added to the observed radial velocity for a correction, but the correction is acceptable only if the difference between the corrected and reference radial velocities is within the threshold of $\pm\max(0.25v_N$, 6 m $s^{-1})$. This threshold is more stringent than the commonly used threshold of $\pm 0.5v_N$ (Hennington, 1981; James and Houze, 2001; Gong et al., 2003). If this threshold is no satisfied, then the date point is flagged for the subsequent check in the next step. All the observations passed the reference check within the cut-off radial ranges (30 km for $\theta \approx 0.5^\circ$ and 80 km for $\theta \geq 1^\circ$) will be treated as seed data for the block-to-point continuity check in the next step.

2.2. *Second Step – Block-To-Point Continuity Check*

In this second step, a block-to-point continuity check is used to replace the point-to-point continuity check in the third step of the three-step dealiasing method. The basic idea is to use the averaged value of non-flagged seed data (instead of or in addition to the single nearest seed datum in each direction, backward along the beam or circle) for the continuity check. The check is processed circle-by-circle from the smallest circle to the largest circle on each tilt. Each circle is checked through four sub-steps. The first three sub-steps go clockwise along the circle (starting from ϕ = 0) and the last sub-step goes counterclockwise along the circle (starting from ϕ = 0). No action is taken at a non-flagged data point. The real action of check applies only to each and every flagged data point.

The first sub-step is designed to search for non-flagged seed data backward from the current circle toward the radar up to 40 gates (10 km, not including the gate at the current circle) along each of the 11 beams in the ±5° vicinity of the identified flagged data point. If there are 40 or more seed data, then their averaged value can be used for the continuity check. To eliminate possible false dealiasing, each dealiased datum in the first sub-step is doubly checked with the nearest seed datum in each direction in the subsequent three sub-steps. These three sub-steps are designed to search for the nearest seed data backward (up to 10 gates) along the current beam, backward (up to 5°) along the current circle, and forward (up to 5°) along the previous circle, respectively. The detailed aspects of these sub-steps are reported in Xu *et al*. (2009a).

After the above last sub-step goes through the entire circle, all the de-flagged data point are turned into new seed data points on the current circle. The process then goes to the next circle (with the radial range distance r increased by one radial range space Δr) until it goes through the entire tilt, and the entire process goes from the highest to the lowest tilt through the entire volume.

3. ILLUSTRATIVE EXAMPLE

For briefness, only one example is given below to show the effectiveness of the new method in this section. Fig. 1a is the image of raw radial velocities scanned at θ = 0.5° by the operational KMHX radar at 201546 UTC on 18 September 2003 from the hurricane Isabel near Drum Inlet, North Carolina. The spatial resolutions of the scans were 250 m in the radial direction and 1° in the azimuthal direction. At

this time, the hurricane center (marked by the blue letter C in Fig. 1a) was about 120 km to the north (in the direction of $\phi \approx 350^{o}$) of the KMHX radar. Even though the Nyquist velocity was as large as $v_N = 23.19$ m s^{-1}, the observed radial velocities were severely aliased in the two main areas (marked by the two white letters A in Fig. 1a). One is the green area to the east of the hurricane center, and the other is the red area to the southwest of the hurricane center. In addition to the above two main areas, the observed radial velocities were also aliased in the three banded green areas to the east of the radar within 80 km radial range, and in a narrow red area to the west of the radar within 90 km radial range. The above aliased velocities were caused by the intense rotational winds around and outside the hurricane eye.

As explained in section 2.1, the reference check goes from the smallest radial range up to r = 30 km only on the lowest tilt ($\theta = 0.5^{o}$), and the 30 km range circle is shown by the white circle in Fig. 1b. Within this 30 km range circle, the aliased radial velocities in the red area to the northwest of the radar and in the green areas to the northeast and east of the radar in Fig. 1a are corrected in Fig. 1b. The corrections are made largely by the reference check in the first step, as revealed by the partially dealiased image produced at the end of the first step (not shown). The dealiased image outside the 30 km range circle in Fig. 1b is produced solely by the block-to-point continuity check in the second step. By comparing Fig. 1b with Fig. 1a, it is easy to see that the aliased radial velocities in the two main alias areas (marked by the two white letters A in Fig. 1a) are all corrected by the block-to-point check in the second step. In addition, the aliased radial velocities in the banded green areas to the east of the radar within 80 km radial range in Fig. 1a are also all corrected.

By comparing Fig. 1b with Fig. 1a outside the 30 km range circle, we also see that the block-to-point continuity check can go through (or around) most data holes. The point-to-point continuity check in the previous three-step method (Gong *et al.* 2003) or in the operationally used method (Eilts and Smith, 1990), however, fails to pass through some large data holes or even occasionally produces false dealiasing (see Figs. 1c and 1d). In terms of passing through data holes and avoiding false dealiasing, the block-to-point continuity check performs significantly better and more robust than the point-to-point continuity check. The improvement attributes to the design of the block-to-point continuity check (see section 2.2), although the design is neither intended nor possible to correct all the aliased radial velocities and leave no flagged data points. Similar improvements are seen from the dealiased images (not shown) on all the remaining tilts above $\theta = 0.5^{o}$.

Because the new dealiaing method is developed for radar data assimilation applications, avoiding false dealiasing is the most important requirement for the design of the new dealiasing method. To meet this requirement, stringent threshold conditions are used for alias corrections in the design of the block-to-point continuity check (see section 2.2), so the completeness of alias corrections is more or less compromised. In particular, the block-to-point continuity check is not able to de-flag data points in an isolated data island or nearly-isolated data peninsular (stretched toward the radar) surrounded by extensive data void areas. Because of this, the data points in the spike-shape data peninsular from $r \approx 35$ to 110 km to the west of the radar in Fig. 1a remain to be flagged and thus blacked in Fig. 1b. This data peninsular contains both aliased radial velocities (in the narrow red area to the west of the radar within 90 km radial range in Fig. 1a) and non-aliased radial velocities (in the extended green area over the radial range from 80 to 110 km to the west of the radar in Fig. 1a). Another flagged (and thus blacked) data area is the nearly disconnected segment of hurricane eyewall image along the southern rim of the hurricane eye in Fig. 1a.

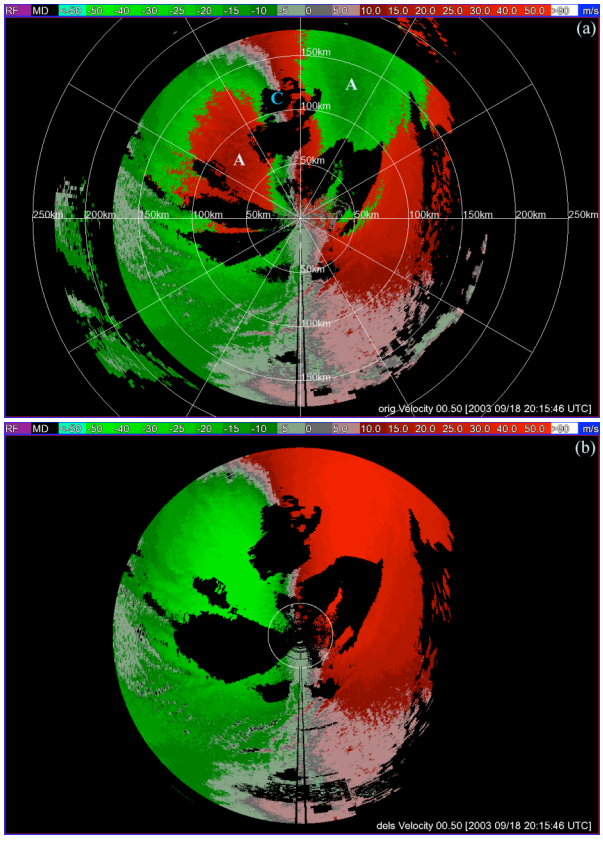

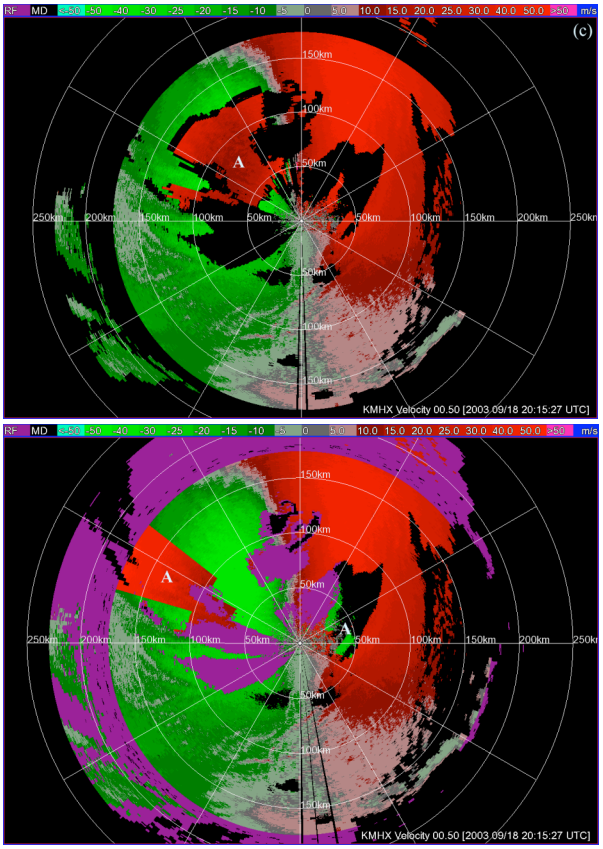

Fig. 1. (a) Raw level-II Doppler radial-velocity image on 0.5° elevation from KMHX radar at 2015 UTC 18 Sept. 2003. (b) Dealiased radial-velocity image by the new method. (c) Dealiased radial-velocity image by the three-step method (Gong *et al.* 2003). (d) Dealiased radial-velocity image by the operational method (Eilts and Smith, 1990).

For the hurricane case exemplified in this section, the completeness of alias corrections can be further improved by relaxing the cut-off radial range for the reference check in the first step. In particular, if the cut-off radial range is extended from 30 to 50 km, then the flagged data points in the blacked area marked by b1 in Fig. 1b can be correctly de-flagged up to r = 50 km by the reference check in the first step and then to the full radial range of the spike-shape data peninsular by the block-to-point continuity check in the second step without causing any false dealiasing (not shown). Although relaxing the cut-off radial range for the reference check can further improve the completeness of alias corrections in this and many other cases, it can also occasionally cause false dealiasing. To avoid false dealiasing, it is necessary to impose a short (30 km) cut-off radial range on the lowest tilt ($\theta \approx 0.5^{o}$) and a limited (80 km) cut-off radial range on the remaining tilts ($\theta \geq 1^{o}$) for the reference check in the first step. As explained in section 2.1, the cut-off radial ranges used in this paper are tuned and selected based on our extensive tests of the new method (as mentioned at the beginning of this section).

4. REFINEMENAT FOR VCP31

The new method has been tested extensively and successfully with real-time radial velocities scanned by the KTLX radar under various weather conditions. It can use the radial velocities estimated by the alias-robust VAD analysis for the reference check in most cases, except for severe winter storms scanned by using the VCP31 mode with the Nyquist velocity reduced below 12 m s^{-1}. In the latter case (VCP31), the reference radial velocities produced by the alias-robust VAD analysis do not have the required horizontal variability (relative to the storm wind) to ensure the reference check to be absolutely free of false dealiasing.

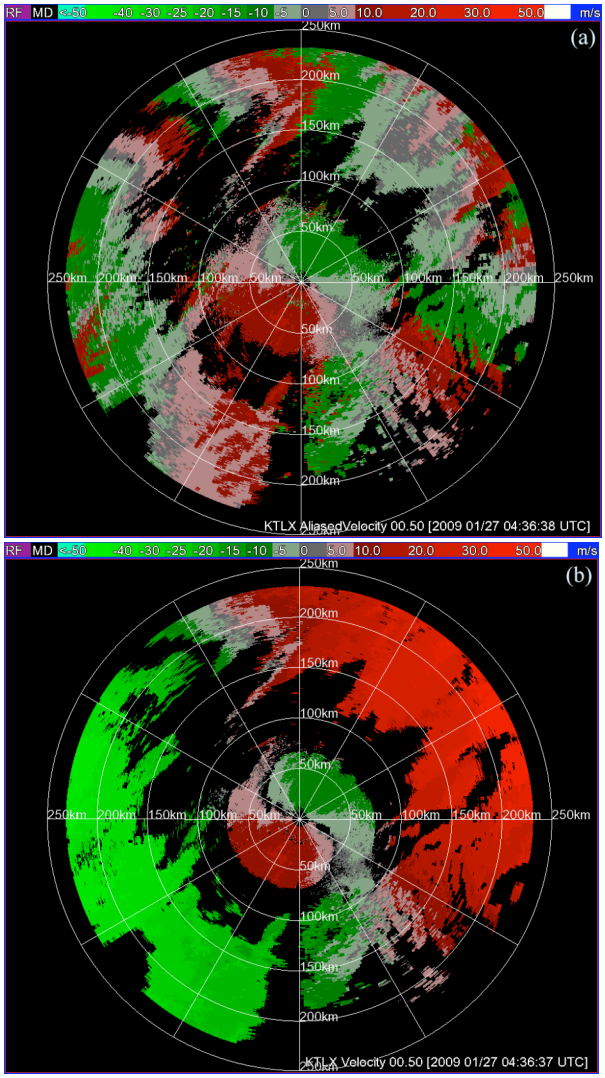

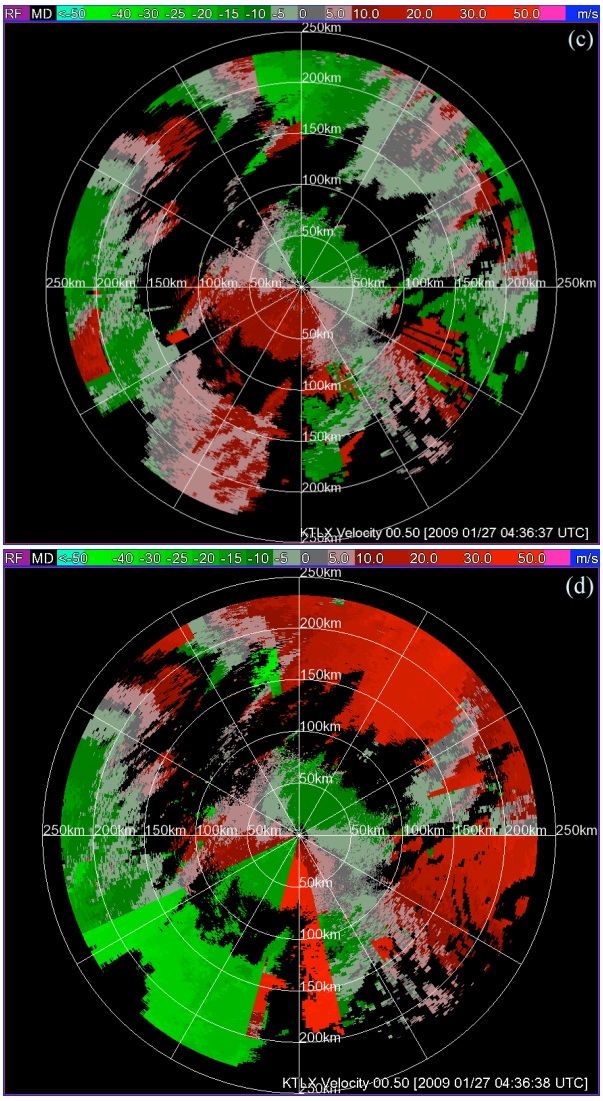

Fig. 2. (a) Raw radial-velocity image scanned by the KTLX radar with VCP31 mode and Nyquist velocity = 11.51 m s^{-1} at 0.5° tilt for the Oklahoma ice storm at 043637 UTC on 27 January 2009. (b) Dealiased radial-velocity image by the further upgraded method. (c) Dealiased radial-velocity image by the three-step method. (d) Dealiased radial-velocity image by the operational method.

To solve the above problem with VCP31, the alias-robust variational analysis (Xu *et al.*, 2009c; section 3.2) is used in place of the alias-robust VAD analysis for the reference check. This further upgrades the method and makes it VCP-adaptive and free of false dealiasing even for VCP31 with a small Nyquist velocity. As shown by the example in Fig. 2, the further upgraded method can correct almost all the alias errors without any false dealiasing, even though the raw radial velocities were severely aliased due to the strong wind and small Nyquist velocity. The three-step method and the operationally used method, however, cannot be free of false dealiasing (see Figs. 2c and 2d).

5. SUMMARY

A new dealiasing method is developed for radar radial-velocity data quality control. The new method not only upgrades but also simplifies the previously developed three-step dealiasing method in three major aspects. First, an alias-robust VAD algorithm is used in place of the modified VAD method for the preliminary reference check in the first step. Second, the alias-robust VAD analysis makes the traditional VAD analysis and refined reference check unnecessary, so the original second step is removed. Third, a block-to-point continuity check procedure is developed to replace the point-to-point continuity check in the original third step. The improved performance and robustness of the new method are exemplified by the result tested with a hurricane case in this paper.

The new method has been tested extensively and successfully with aliased radial-velocity observations collected under various weather conditions in the central United State by six NOAA/NWS operational radars (KINX, KLZK, KSGF, KSRX, KTLX and KVNX) during 20-28 May 2005. The method has been also successfully tested with severely aliased radial-velocity data collected under hurricane high-wind conditions. These include data collected (i) by KAKQ, KMHX and KRAX radars from the long-lived hurricane Isabel that made landfall near Drum Inlet, North Carolina on 18 September 2003, (ii) by FLIX, KMOB and KEVX radars from the hurricane Katrina that caused the most devastating disaster in New Orleans, Louisiana, on 29 August 2005, and (iii) by KHGX radar from the hurricane IKE that passed over Houston, Texas, on 13 September 2008. Recently, the method is further upgraded (see Fig. 2). This further upgraded method is being incorporated (in place the previous three-step method) into the automated quality control package for operational radar data assimilation applications at NCEP.

Acknowledgments.
The research work was supported mainly by the NSSL-NCEP radar data quality control project and by the ONR Grant N000140410312 to the University of Oklahoma. Funding was also provided to CIMMS by NOAA/Office of Oceanic and Atmospheric Research under NOAA-University of Oklahoma Cooperative Agreement #NA17RJ1227, U.S. Department of Commerce.

REFERENCES

Eilts, M. D., and S. D. Smith, 1990: Efficient dealiasing of Doppler velocities using local environment constraints. *J. Atmos. Oceanic Technol.*, **7**, 118–128.

Gong, J., L. Wang, and Q. Xu, 2003: A three-step dealiasing method for Doppler velocity data quality control. *J. Atmos. Oceanic Technol.*, **20**, 1738–1748.

Hennington, L., 1981: Reducing the effects of Doppler radar ambiguities. *J. Appl. Meteor.*, **20**, 1543–1546.

James, C. N., and R. A. Houze, 2001: A real-time four-dimensional Doppler dealiasing scheme. *J. Atmos. Oceanic Technol.*, **18**, 1674–1683.

Liu, S., G. DiMego, K. V. Kumar, D. Keyser, S. Guan, Q. Xu, K. Nai, P. Zhang, L. Liu, J. Zhang, X. Xu, and K. Howard, 2009: WSR-88D radar data processing at NCEP. *34rd Conference on Radar Meteorology*. Williamsburg, VA, Amer. Meteor. Soc., CD-ROM, 14.2.

Liu, S., Q. Xu, and P. Zhang, 2005: Quality control of Doppler velocities contaminated by migrating birds. Part II: Bayes identification and probability tests. *J. Atmos. Oceanic Technol.*, **22**, 1114–1121.

Liu, S., P. Zhang, L. Wang, J. Gong, and Q. Xu, 2003: Problems and solutions in real-time Doppler wind retrievals. Preprints, *31th Conference on Radar Meteorology*, Seattle, Washington, Amer. Meteor. Soc., 308-309.

Tabary, P., G. Scialom, and U. Germann, 2001: Real-time retrieval of the wind from aliased velocities measured by Doppler radars. *J. Atmos. Oceanic Technol.*, **18**, 875–882.

Xu, Q., K. Nai, L. Wei, P. Zhang, S. Liu, and D. Parrish, 2009a: A VAD-based dealiasing method for radar velocity data quality control. *J. Atmos. Oceanic Technol.* (to be submitted).

Xu, Q., K. Nai, and L. Wei, 2009b: Fitting VAD winds to aliased Doppler radial-velocity observations – a global minimization problem in the presence of multiple local minima. Submitted to *Quart. J. Roy. Meteor. Soc.*

Xu, Q., K. Nai, L. Wei, and Q. Zhao, 2009c: An unconventional approach for assimilating aliased radar radial velocities. *Tellus*, **61A**, in press.

Xu, Q., K. Nai, L. Wei, P. Zhang, L. Wang, H. Lu, and Q. Zhao, 2005: Progress in doppler radar data assimilation. *32nd Conference on Radar Meteorology*, Albuquerque, New Mexico, Amer. Meteor. Soc., CD-ROM, JP1J7.

Zhang, P., S. Liu, and Q. Xu, 2005: Quality control of Doppler velocities contaminated by migrating birds. Part I: Feature extraction and quality control parameters. *J. Atmos. Oceanic Technol.*, **22**, 1105-1113.